Supplemental Material for "Exploring the potential of MB_2 MBene family as promising anodes for Li-ion batteries"

Ying Han[a], Lianli Wang[a*], Bin. Zheng [a], Jinlei Wang [a], Li Zhang[a], Beibei Xiao[b]

[a]*School of Materials Science and Engineering, Xi'an University of Science and Technology, Xi'an 710054, PR China*

[b]*School of Energy and Power Engineering, Jiangsu University of Science and Technology, Zhenjiang, Jiangsu, 212003, PR China*

Structural dynamic stability can be used to evaluate the properties of 2D materials. Here, we calculate the phonon spectrum using the finite displacement method. The phonon spectra of CrB_2, CuB_2, ZnB_2, YB_2 and NiB_2 have more virtual frequencies and are not suitable for use as negative electrode materials for LIBs. The phonon spectrum of TiB_2, VB_2, HfB_2 and NbB_2 is calculated, and there is no virtual frequency in the phonon spectrum curve. The dynamic stability of these four materials was proved.[1] FeB_2 and MnB_2 have previously been reported as anode materials for LIBs.[2, 3] CoB_2 and ZrB_2 are distorted in the optimization process, and their structures are easy to collapse, which are not suitable for the LIBs anode materials. Therefore, we won't conduct additional calculations for FeB_2, MnB_2, CoB_2 and ZrB_2.

In order to better understand the electronic properties of the MB_2 monolayer, we calculated the band structure of MB_2 monolayer. The ScB_2, TiB_2, VB_2, NbB_2, MoB_2 and WB_2 monolayers exhibit metallicity due to the Fermi energy level crossing the valence band (Fig. S6). Their Dirac cones lying above the Fermi level suggest their potential for experimental preparation. As shown in Fig. S6(g), the band structure of HfB_2 exhibits non-metallic properties and is not suitable for LIBs electrode materials.

* Corresponding author E-mail: wanglianli@xust.edu.cn

Table S1 The “Layer thickness” represents the distance between the B-layer and the M-layer.

MBenes	Layer thickness(Å)
ScB_2	1.409
YB_2	1.682
TiB_2	1.189
ZrB_2	0.079
HfB_2	1.348
VB_2	0.997
NbB_2	1.738
TaB_2	1.466
CrB_2	0.878
MoB_2	1.574
WB_2	1.607
MnB_2	0.739
FeB_2	0.625
CoB_2	0.433
NiB_2	0.995
CuB_2	1.055
ZnB_2	1.730

Table S2 The corresponding adsorption energy of Li atom at different optimal sites on the surface of MBenes (Unit: eV)

MBenes	Site 1	Site 2	Site 3	Site 4	Site 5	Site 6
ScB_2	-1.87	-1.00	-1.09	-0.17	-0.29	-0.27
TiB_2	-0.92	-0.08	-0.14	0.207	0.06	0.07
VB_2	-0.77	0.02	0.01	-0.10	-0.32	-0.31
CrB_2	-0.87	0.18	0.20	0.01	-0.21	-0.20
MnB_2	-0.11	-0.02	0.01	-0.43	-0.80	-0.84(move to site 5)
FeB_2	0.22	0.22	0.29	-0.28	-0.63	-0.57
CuB_2	-2.16	-1.33	-2.11	0.36	-0.31	-0.19
ZnB_2	-1.74	-1.26	-1.74(move to site 1)	-0.29	-0.48	-0.48
YB_2	-2.10	-2.07	-2.10	-0.12	-0.19	-0.18
NbB_2	-1.01	-0.23	-0.28	0.84	0.79	0.77
MoB_2	-2.30	-1.60	-2.31(move to site 1)	-0.85	-1.01	-0.99
HfB_2	-1.71	-0.83	-1.71(move to site 1)	-0.30	-0.48	-0.46
TaB_2	-2.25	-1.38	-2.24	-0.86	-0.96	-0.95
WB_2	-1.96	-1.24	-1.96(move to site 1)	-0.62	-0.86	-0.83

Table S3 The amount of charge transfer of the Li, B, and M atoms at the most stable adsorption position of the Li atom is determined by Bader charge analysis. (M=Sc, Ti, V, Cr, Mn, Fe and Cu)

ΔQ(e)/atom	ScB_2	TiB_2	VB_2	CrB_2	MnB_2	FeB_2	CuB_2
M1	-1.037	-1.028	-0.900	-0.694	-0.375	-0.119	-0.300
M2	-1.040	-1.034	-0.897	-0.700	-0.376	-0.121	-0.296
M3	-1.040	-1.036	-0.897	-0.701	-0.375	-0.122	-0.296
M4	-0.852	-0.979	-0.855	-0.671	-0.312	-0.027	-0.305
B1	0.537	0.596	0.519	0.456	0.420	0.137	0.326
B2	0.612	0.692	0.482	0.369	0.281	0.201	0.241
B3	0.674	0.605	0.602	0.467	0.410	0.267	0.170
B4	0.584	0.660	0.576	0.422	0.116	0.022	0.203
B5	0.626	0.659	0.570	0.423	0.138	0.021	0.279
B6	0.651	0.511	0.639	0.465	0.339	0.269	0.169
B7	0.534	0.600	0.518	0.548	0.340	0.140	0.405
B8	0.591	0.599	0.483	0.456	0.261	0.205	0.244
Li	-0.840	-0.845	-0.841	-0.838	-0.866	-0.874	-0.840

Table S4 The amount of charge transfer of the Li, B, and M atoms at the most stable adsorption position of the Li atom is determined by Bader charge analysis. (M=Zn, Y, Nb, Mo, Hf, Ta and W)

ΔQ(e)/atom	ZnB_2	YB_2	NbB_2	MoB_2	HfB_2	TaB_2	WB_2
M1	-0.327	-0.929	-0.616	-0.442	-1.031	-0.730	-0.501
M2	-0.316	-0.921	-0.619	-0.434	-0.840	-0.734	-0.506
M3	-0.418	-0.921	-0.620	-0.437	-1.053	-0.740	-0.494
M4	-0.401	-0.701	-0.564	-0.414	-1.060	-0.686	-0.479
B1	0.191	0.463	0.288	0.387	0.642	0.617	0.242
B2	0.150	0.515	0.382	0.311	0.515	0.531	0.406
B3	0.513	0.662	0.380	0.208	0.598	0.470	0.402
B4	0.363	0.470	0.388	0.390	0.646	0.364	0.423
B5	0.250	0.556	0.386	0.390	0.600	0.399	0.356
B6	0.295	0.651	0.383	0.293	0.604	0.505	0.421
B7	0.076	0.475	0.577	0.210	0.625	0.351	0.267
B8	0.476	0.516	0.479	0.384	0.597	0.495	0.311
Li	-0.851	-0.837	-0.843	-0.845	-0.843	-0.842	-0.849

Table S5 The migration barrier of Li atoms along Path I and Path II. (B side)

MBenes	Path II	Path I-1	Path I-2
ScB_2	0.831	2.386	-
TiB_2	0.809	2.440	0.814
VB_2	0.967	2.836	0.951
CrB_2	0.955	0.001	1.280
MnB_2	0.305	0.733	0.280
FeB_2	0.114	0.006	0.362
CuB_2	0.662	0.751	-
ZnB_2	0.330	0.330	-
YB_2	0.844	3.220	0.841
NbB_2	0.682	2.190	-
MoB_2	0.631	2.145	-
HfB_2	0.903	2.689	0.902
TaB_2	0.732	2.351	-
WB_2	0.604	2.211	-

The "-" is means no transition state is found.

Table S6 The migration barrier of Li atoms along Path III and Path IV. (Metal side)

MBenes	Path IV	Path III-1	Path III-2
ScB_2	0.042	0.020	0.073
TiB_2	0.029	0.037	-
VB_2	0.028	0.337	0.048
CrB_2	0.001	0.151	-
MnB_2	0.001	0.603	-
FeB_2	0.052	0.773	0.070
CuB_2	0.044	0.449	0.006
ZnB_2	0.029	0.451	0.032
YB_2	0.014	0.026	0.117
NbB_2	0.011	0.120	0.070
MoB_2	0.029	0.076	0.030
HfB_2	0.135	0.051	0.018
TaB_2	0.130	0.134	0.117
WB_2	0.029	0.083	0.044

The "-" is means no transition state is found.

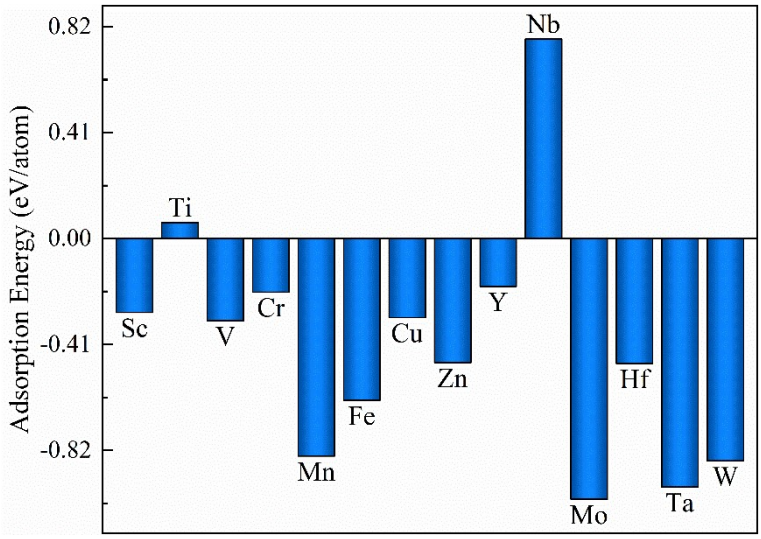

Fig. S1 The adsorption energy of Li atom on metal side of MB_2 monolayers.

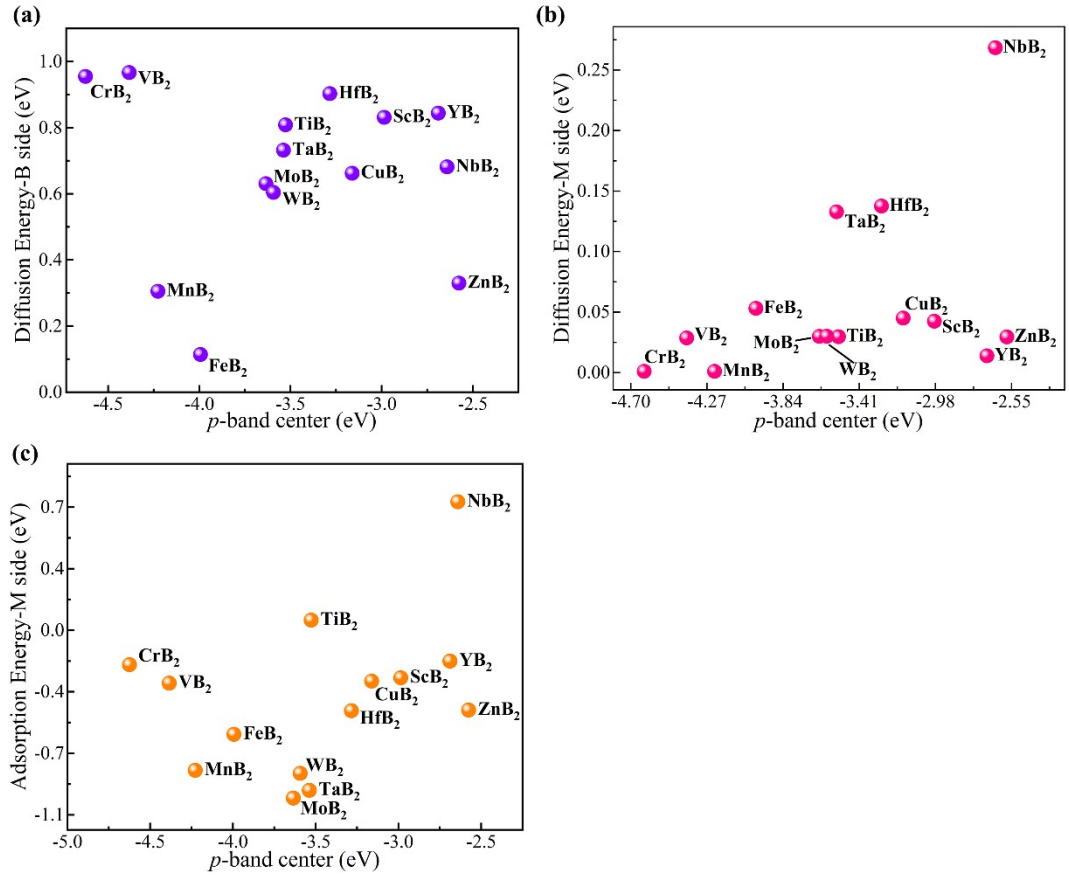

Fig. S2 The relationship between the *p*-band center and (a) the migration energy barrier of Li atom on the B atomic side and (b) the migration energy barrier and (c) the adsorption energy of Li atom on the metal side of MB_2 monolayer.

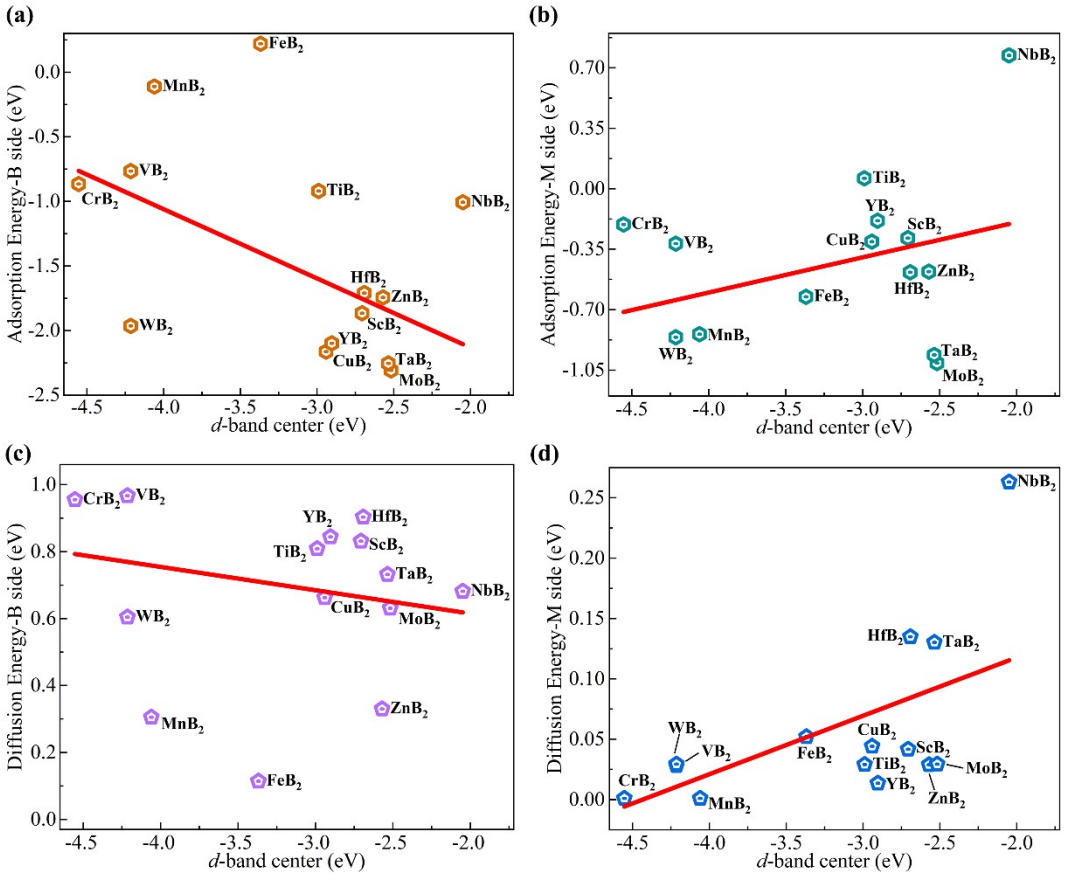

Fig. S3 The relationship between the *d*-band center and the adsorption energy on the (a) B / (b) metal side and the migration energy barrier on the (c) B/ (d) metal side of MB_2 monolayer.

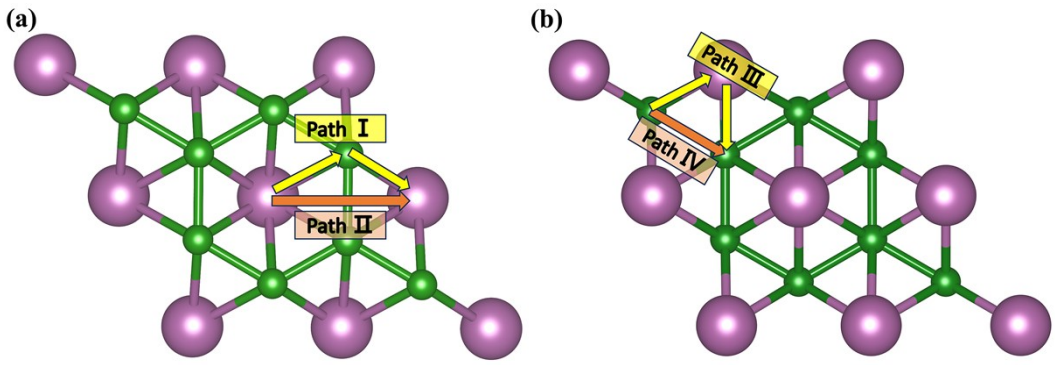

Fig. S4 Possible diffusion paths of Li atom on (a) B atomic side and (b) metal side of MB_2 monolayer. The purple, orange, and green spheres represent the M, Li, B atoms, respectively.

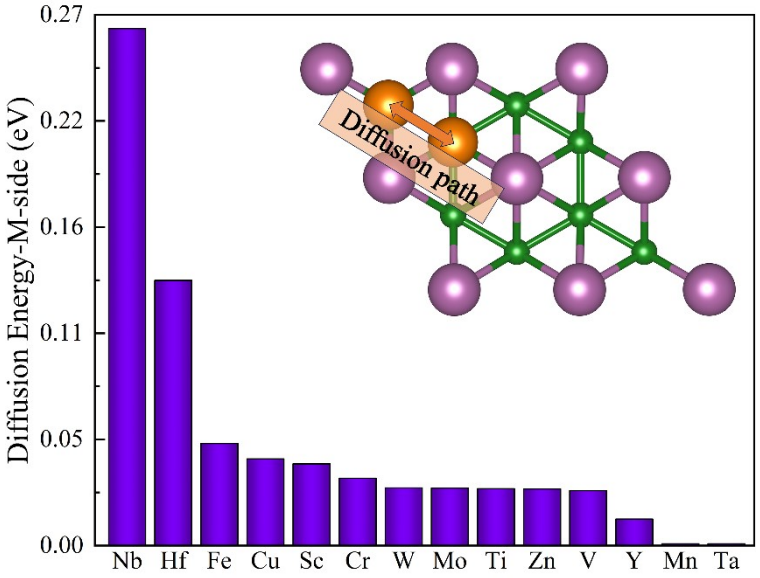

Fig. S5 Diffusion barrier profiles for Li atom and the diffusion path of Li atom on the metal side of MB_2 monolayer. The purple, orange, and green spheres represent the M, Li, B atoms, respectively.

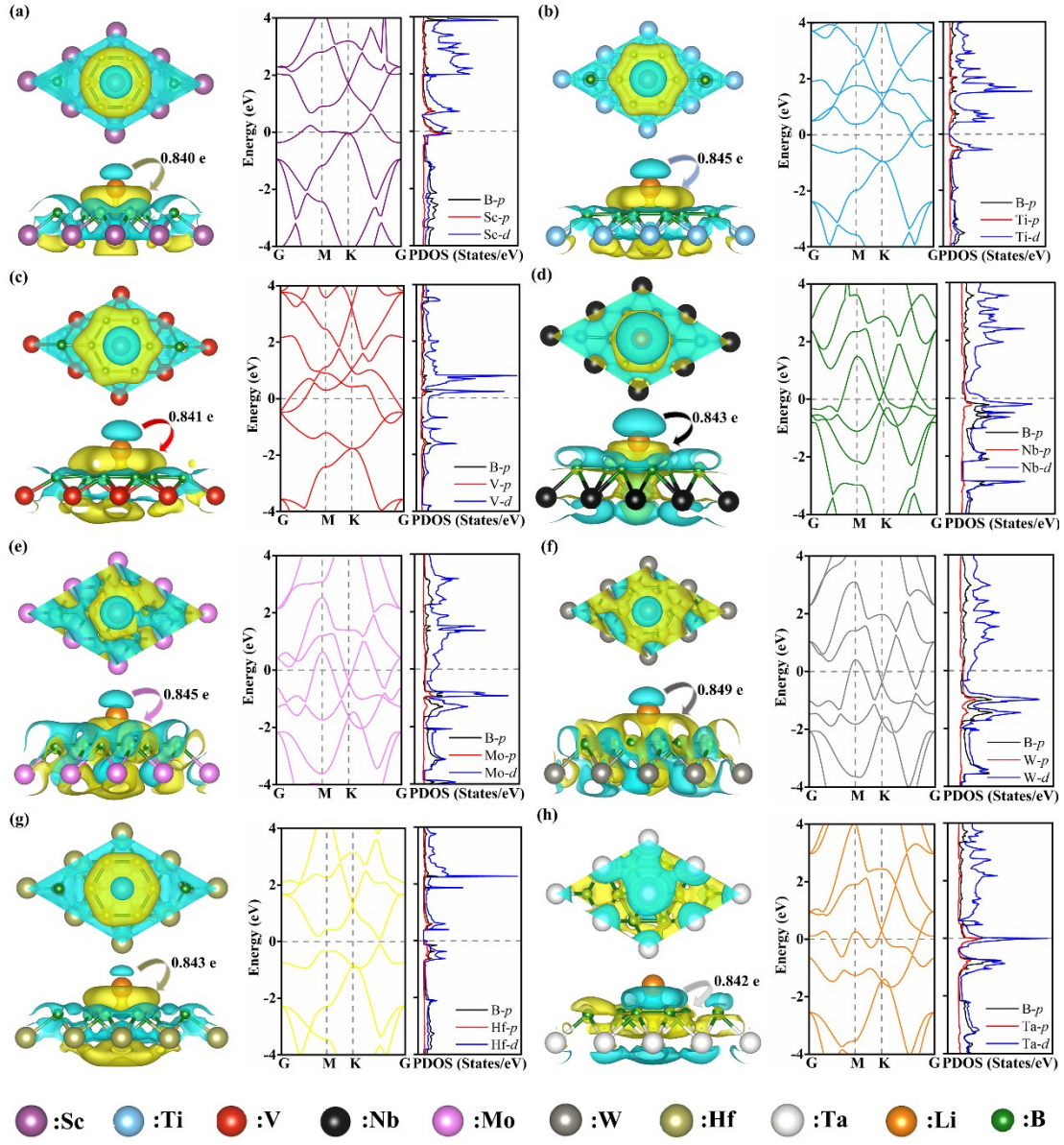

Fig. S6 Charge density difference, band structure and PDOS of Li atom at the most stable adsorption site on MB_2 surface. (M= Sc, Ti, V, Nb, Mo, W, Hf and Ta) The purple, blue, red, black, pink, gray, grass green, white, orange, and green spheres represent Sc , Ti, V, Nb, Mo, W, Hf, Ta, Li and B atoms, respectively.

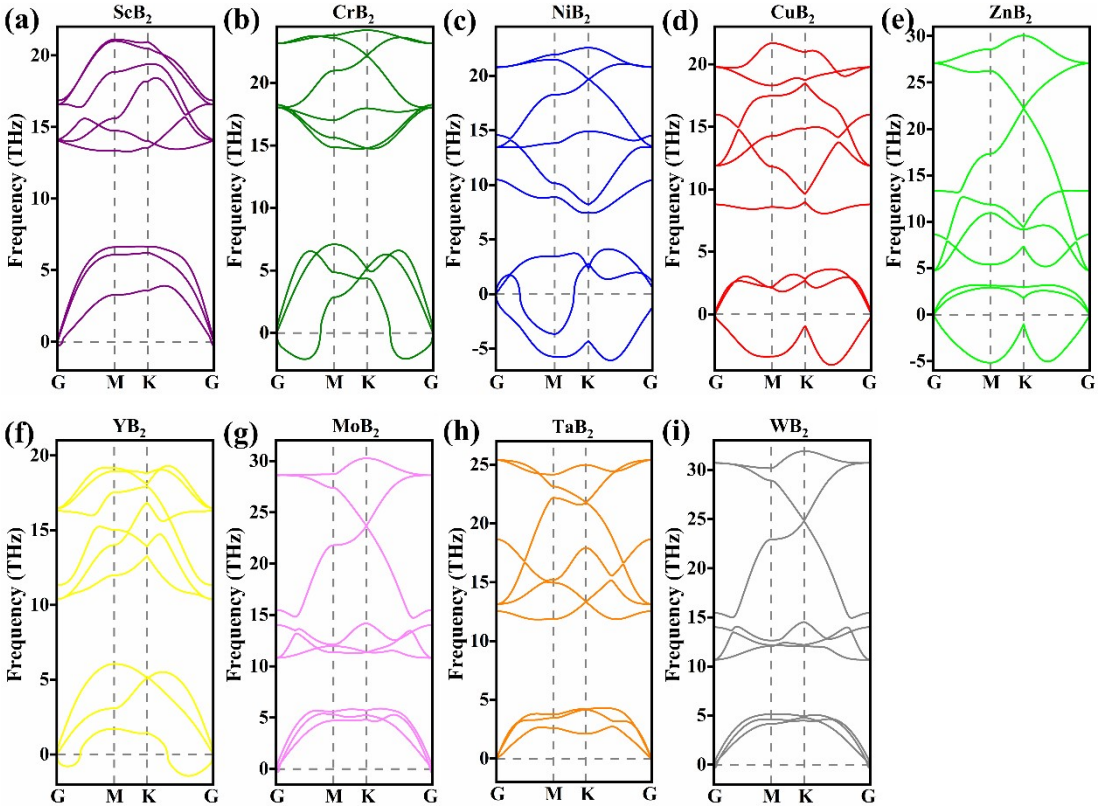

Fig. S7 The phonon dispersion curves of (a) ScB_2, (b) CrB_2, (c) NiB_2, (d) CuB_2, (e) ZnB_2, (f) YB_2, (g) MoB_2 (h) TaB_2 and (i) WB_2.

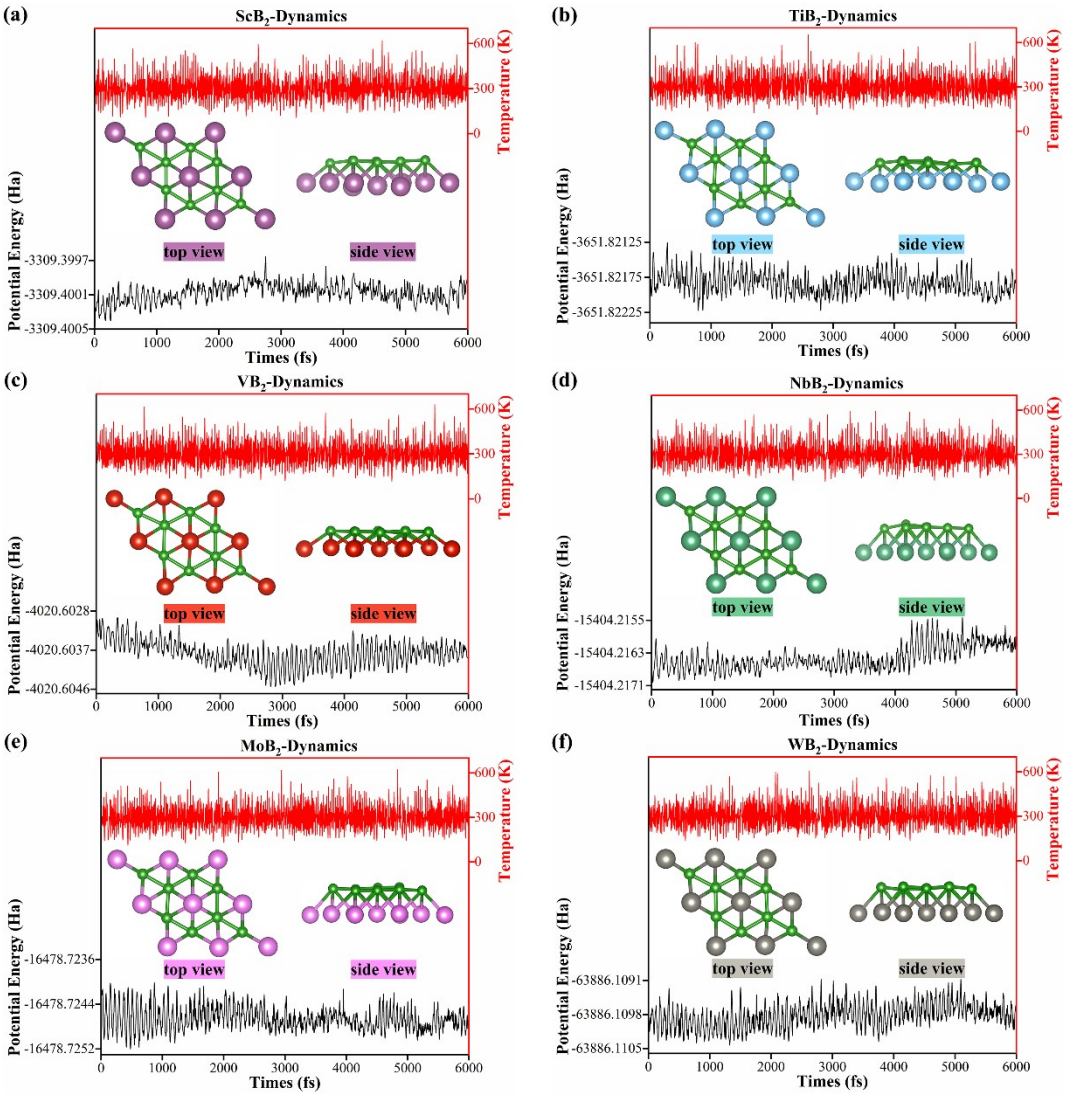

Fig. S8 (a-f)The potential energies and temperatures of the MB_2 (M=Sc, Ti, V, Nb, Mo and W) monolayer were analyzed via AIMD simulations at 300 K, along with the resultant structural evolution observed over a 6.0 ps duration.

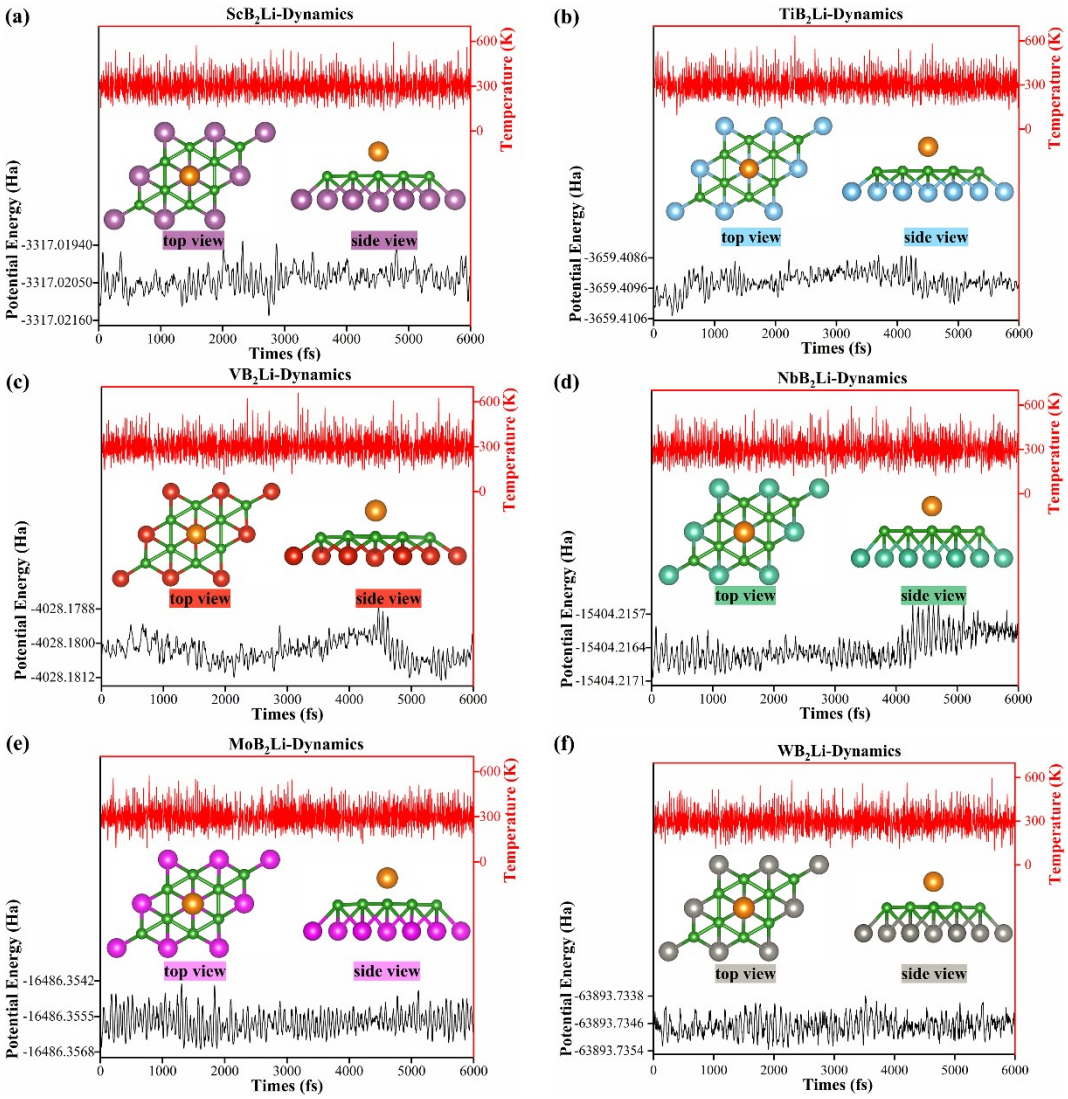

Fig. S9 (a-f)The potential energy and temperature of MB_2 (M=Sc, Ti, V, Nb, Mo and W) monolayers at 300 K after adsorption of a Li atom were analyzed by AIMD simulation, and the structural evolution observed at 6.0 ps duration was also analyzed.

1. C. Zhang, T. He, S. K. Matta, T. Liao, L. Kou, Z. Chen and A. Du, *The Journal of Physical Chemistry Letters*, 2019, **10**, 2567-2573.
2. S. Luo, J. Zhao, Y. Wang, Y. Zhang, Y. Xiong, N. Ma and J. Fan, *The Journal of Physical Chemistry C*, 2023, **127**, 12484-12491.
3. B. Zhang, L. Fan, J. Hu, J. Gu, B. Wang and Q. Zhang, *Nanoscale*, 2019, **11**, 7857-7865.